



## **WestminsterResearch**

<http://www.wmin.ac.uk/westminsterresearch>

### **A case study in the digitisation of a photographic collection.**

**Sophie Triantaphillidou**

**Ralph E. Jacobson**

**Geoffrey G. Attridge**

School of Media, Arts and Design

This is an electronic version of an article published in the Imaging Science Journal, 50. pp. 97-115, 2002.

The Imaging Science Journal is available online at:

[www.ingentaconnect.com/content/maney](http://www.ingentaconnect.com/content/maney)

---

The WestminsterResearch online digital archive at the University of Westminster aims to make the research output of the University available to a wider audience. Copyright and Moral Rights remain with the authors and/or copyright owners. Users are permitted to download and/or print one copy for non-commercial private study or research. Further distribution and any use of material from within this archive for profit-making enterprises or for commercial gain is strictly forbidden.

---

Whilst further distribution of specific materials from within this archive is forbidden, you may freely distribute the URL of WestminsterResearch.  
(<http://www.wmin.ac.uk/westminsterresearch>).

In case of abuse or copyright appearing without permission e-mail [wattsn@wmin.ac.uk](mailto:wattsn@wmin.ac.uk).

# **A Case Study in Digitising a Photographic Collection**

S. Triantaphillidou, R. E. Jacobson and G. G. Attridge

Imaging Technology Research Group, University of Westminster,  
School of Communication and Creative Industries, Harrow Campus,  
Watford Road, Northwick Park, Harrow HA1 3TP

Paper presented at The Royal Photographic Society , Imaging Science Group  
Annual Conference: Digital Futures 2000,  
University of Westminster, London, September 2000

## **Abstract**

This paper reviews the processes involved in the digitisation, display and storage of medium size collections of photographs using mid-range commercially available equipment. Guidelines for evaluating the performance of these digitisation processes based on aspects of image quality are provided. A collection of photographic slides, representing first-generation analogue reproductions of a photographic collection from the nineteenth century, is treated as a case study. Constraints on the final image quality and the implications of digital archiving are discussed. Full descriptions of device characterisation and calibration procedures are given and results from objective measurements carried out to assess the digitisation system are presented. The important issues of file format, physical storage and data migration are also addressed.

## **1. Introduction**

Photographs are artistic media, information carriers and historical documents. Their collection and storage is undertaken by numerous establishments throughout the world and millions of images are held, either in official archives or, kept by individuals in various storage conditions [1]. Photographic materials, however, are not permanent records but are subject to slow decay processes which cannot be avoided completely, even under ideal storage conditions. Generally, conditions that favour of the preservation of photographs, such as limited handling and avoidance of exposure to light and other deleterious ambient conditions [2] are against the very essence of a photographic collection. Digital image databases and archives are obvious steps towards easy communication, exchange and lossless duplication of photographs, enabled by modern technology. Also, the digitisation of photographs provides a means of re-constructing faded or damaged images [3].

The digitisation of many organised art collections has taken place in the last ten years [4-6]. In the majority of these projects large amounts of money, time and manpower were invested to ensure adequate quality. Large budgets, however, may not be available in establishments which have needs for digitising their images. This paper concentrates on the processes involved in the digitisation, display and storage of medium size collections of photographs, using mid-range commercially available equipment. A photographic collection of approximately seven hundred 35mm transparencies is treated as a case study. This collection comprises first-generation analogue copies of images, belonging originally to the

photographic collection of William Henry Fox Talbot<sup>1</sup>. Today the original photographs are part of the precious photographic archive of the Royal Photographic Society (RPS) and are currently located in Bath, UK. The original Talbot collection has been rarely viewed and cannot be exhibited due the detrimental effects of handling and damage from exposure to light. These problems of access encouraged the RPS to produce copies on 35mm Kodak Ektachrome transparency film five years ago. Analogue copies, however, also require appropriate storage for maximum life expectancy (imperative in this case, where every time a photographic copy is made, additional damage to the original might be introduced). In addition they do not offer as many advantages in accessing the collection when compared with digital reproductions.

## **2. Image quality and aims for the digitisation**

A crucial concern in the digitisation of photographs is the quality delivered by the reproduction system. Acceptable image quality varies from application to application, amongst observers, image content and viewing conditions. To evaluate the quality of the digital reproductions, it is necessary to understand whether and how the digital imaging system degrades original image information and how important this image distortion is to the Human Visual System (HVS). Photographic images contain a high density of information, and require very high quality digitising procedures to retain all their characteristics. Before starting the digitisation process, it is therefore essential to define the purpose of digitisation and the uses of the acquired images [7,8]. Quality criteria may then be established. Frey *et al.* [7] have laid out goals as well as quality issues for the digitisation of photographic collections. Frey [8] has also listed rendering intents that apply when digitising original artwork.

In this work the issue of accessibility was of a major importance. The immediate aim was to make the collection available to scholars, researchers and visitors, as well as to educational institutions, by introducing an easily accessible, high quality digital version of the archived material. Furthermore, the collection would be rendered in such a way that the reproduced images would approach the present appearance of the photographs. There was no intention of reconstructing digitally the original photographs or eliminating ageing artefacts. The digitisation process involved the production of high spatial resolution digital image files from photographic copies. A number of reasons led to the decision to digitise the slide copies instead of the original photographs. These included: the prevention of potential harm to the

---

<sup>1</sup> Talbot, 'the father of modern photography', is the inventor of the negative-positive photographic process.

originals due to light exposure during scanning and scanners being designed primarily for digitising modern media. The primary output device for delivering the digital archive was to be the cathode ray tube (CRT) display system. The future uses of a digital archive, however, cannot be predetermined and a digital archive should not be optimised for a specific output [9]. Limitations in the colour resolution of the acquisition device, and the need for immediate output via common commercial applications forced us to select this primary output device, although the high spatial resolution of the digital images would allow reproductions on film and prints up to A4 size.

A description of the imaging stages involved in the development of the digital collection of photographs is illustrated in Figure 1. The steps investigated in this work are the image acquisition and post-acquisition processes, the display and the physical storage of the images. It was decided that the first generation analogue reproductions would be treated as the originals, therefore any quality associations are made between the slides and the digital reproductions. Aspects of image quality are investigated by implementing objective measurements, known to be consistent with the HVS [10]. Information on the distribution system and the user interface are described elsewhere [1, 11].

### **3. Digital image acquisition**

After a review of previous projects and an extended market survey on digital image acquisition a Nikon LS-1000 35mm slide scanner was selected for use in this project. There are several advantages in using a scanning system for the reproduction of original photographs [12]. Amongst them, the most essential is that a linear CCD imager, used in scanning systems, has a less demanding architecture than that of the two-dimensional CCD devices incorporated in digital still cameras and thus less artefacts resulting from pixel size inhomogeneity, current transfer, etc. are present.

The scanner operates as follows: Red, green and blue light is flashed, one at a time, from a light emitting diode (LED) array. A transmitted spectrum - for each flash - results when the incident light is selectively absorbed as it passes through the film layers and the optical system of the device. The linear monochrome CCD array of 2592 active photoelements scans the image plane sequentially. The resulting CCD voltages are scaled and converted to digital values, dedicating 12 bits per colour channel. The 12-bit digital signal is optimised by the device and down-sampled to 8 bits for output. The overall spectral responses of the red, green and blue channels are determined by: the spectral distribution of the LEDs,  $I(\lambda)$  the spectral transmittance of the optical lenses,  $T_o(\lambda)$  the sensitivity of the CCD detector,  $D(\lambda)$  (i.e. all the

factors affecting the response of the device), and the spectral transmittance of the specific film,  $T_f(\lambda)$ . The spectral response for the  $i^{\text{th}}$  channel  $S_i(\lambda)$ , is given by Equation 1:

$$S_i(\lambda) = \int I_i(\lambda) T_{oi}(\lambda) D_i(\lambda) T_{fi}(\lambda) d\lambda \quad (1)$$

The scanner is capable of scanning transparent originals of up to 24.3 mm by 36.5 mm. At the optical resolution (resolution applied in the digitisation of the collection) the device yields maximum image dimensions of 2592 by 3888 square pixels, of approximately 9.4  $\mu\text{m}$  x 9.4  $\mu\text{m}$  size [13], resulting in 28.8 MB colour digital image files. Scanning test patterns of known physical size confirmed these pixel dimensions experimentally [14]. These dimensions correspond to the horizontal and vertical sampling intervals achieved at this resolution (i.e. pixel pitch). The useful bandwidth of the scanner is dictated by the sampling theorem [15]. The maximum spatial frequency sampled faithfully is given by the Nyquist frequency ( $1/2\delta x$  where  $\delta x$  is the sampling interval), being 53.2 cycles per mm. This, however, does not cover the entire bandwidth of high-resolution photographic films, such as the Ektachrome 100 ISO used in the project, having a cut-off frequency of 100 cycles per mm (determined by extrapolating the spatial frequency response curves provided by Kodak [16]). Beyond the Nyquist limit, aliasing occurs which may be prevented in modern scanners by the use of anti-aliasing filters [17].

The voltage output of the CCD of the scanner is quantized initially to 12 bits per colour component, providing 4096 code levels and theoretically covering a density range of 3.6 which approximates to the density range of slide films. Electronic noise and quantization noise reduce the dynamic range of the scanner. Flare due to light scattering via the optical system reduces the illuminant range. The tonal range of the reproduction, being approximately 2.7 to 3.0 density units, is therefore compressed and optimised by the device and/or according to the scanner's settings. In the digitisation of original artwork the loss in dynamic range is a serious disadvantage and unless the data contain the full dynamic range of the original, the digital archive is inferior to the stored transparencies [16].

### 3.1. Tone reproduction

The tonal characteristics of scanners are described by the relationship between input transmittance (or reflectance) or input density and the generated digital counts. Although most such systems respond linearly to intensity and therefore to transmittance, the transfer function of the Nikon LS-1000 can be presented as a power function (see Equation 2), since

there is a non-linear mapping of the output signal, the form of which depends primarily on the scanner's *gamma settings*:

$$d = k_o + t^{\gamma_s} \quad (2)$$

where  $d$  is the generated normalised (i.e. divided by 255) pixel value,  $k_o$  is the system offset and  $t$  is the film transmittance. The exponent  $\gamma_s$  describes the non-linearity in the contrast of the acquired image. An offset in the positive direction can be caused either by an electronic shift or by stray light in the system. While the electronic offset can be set to zero and offset from uniform stray light can be minimised electronically, signals from flare light (i.e. the stray light coming through the lens) and stray light from the illumination system are often image dependent [17]. Similarly, the scanner's transfer function can be represented by plotting film densities versus the common logarithm of the normalised pixel counts<sup>2</sup>. The resulting transfer curve is similar to the photographic characteristic curve, where gamma ( $\gamma$ ) is the slope of the straight-line portion and is used as a means of quantifying the effective image contrast. The gamma model in Equation 2, being compatible with models of the display and photographic transfer functions [19], can be used to deduce the overall contrast in a hybrid imaging system [20]. Alternatively, the scanner transfer function may be plotted according to the ISO standard 16067-1 [21], that is density versus pixel count, or density versus  $\log_2$  of the pixel count. In the latter case, information on the output bit-depth is obtained. This ISO standard, however, does not define a metric describing the acquired image contrast.

Another important parameter affecting the way the scanner maps the original tones is the specification (manual or automatic) of the white and black points in the original, corresponding to the limits of the reproduction range [22]. Because the dynamic range of the original media often exceeds that of the device, the device's range needs to be used as efficiently as possible. The white and black points were selected, prior to the scanning process, to represent the lightest and darkest points in the image for a specific channel. The available intensity range was then mapped according to those limits.

The scanner's transfer function can be determined by averaging the response of the system to uniform transmittance steps of a conventional greyscale. The resulting curve represents an average response to the specific input target and target positioning [17]. Figures 2 and 3 represent in  $\log_{10}$ - $\log_{10}$  space the RGB and monochrome responses of the scanner to two different test targets, using a *gamma setting* of 1. The first target was the Q-60E3 on Kodak

---

<sup>2</sup> A power relationship appears linear when represented in  $\log_{10}$ - $\log_{10}$  units.

Ektachrome colour transparency film, which includes a 24-step greyscale covering the entire dynamic range of the material. The second was a custom made target on Agfa Scala black-and-white transparency film, comprising a 20-step Kodak greyscale. In both figures it can be seen that only a part of the curves are straight lines which correspond to a range of input densities from approximately 0.3 to 2.2. Effective gamma values, determined from the straight-line portions of the curves, are tabulated in Table 1. They are shown to differ significantly for the two input targets. This is most likely due to the difference in the dynamic range of the targets, resulting essentially in different mapping of the output signal. Figure 4 shows the transfer function of the RGB and monochrome channels when scanning target the Q-60E3, plotted according to the ISO method.

Table 2 shows effective gamma values of the monochrome response, for five different scanner *gamma settings* (see Figure 5 for the respective transfer functions). The effective gamma values indicate that the scanner accounts for the non-linearity of a display and/or a specific application and thus an appropriate gamma-correction is applied to compensate for this non-linearity. The calculated gamma is determined from  $1/(\textit{gamma setting})$ , a functional relationship which describes with enough precision the relationship between the scanner *gamma setting* and the effective gamma for the specific target.

### 3.2 Sharpness

The sharpness of the scanner was assessed by measuring the modulation transfer function (MTF). The overall MTF of the system is given by the product of the MTFs of the detector, optics, and electro-mechanical components. The basic detector MTF,  $M_d(\omega)$ , is defined by the size of the CCD sampling aperture (i.e. the size of the CCD photoelement) :

$$M_d(\omega) = \frac{\sin(\pi\omega x)}{\pi\omega x} \quad (3)$$

where  $x$  is the linear dimension of the aperture and  $\omega$  is the spatial frequency. Equation 3 defines the maximum MTF of the detector, obtained when the centre of the pixel coincides with the optimum recording of the maximum of a signal. There are further characteristics other than the geometric shape of the detector that affect its frequency response, such as mis-diffusion, charge transfer inefficiency, time-delay and integration errors [23].

The optical system of the scanner consists of several lenses with varying focal length, varying indices of refraction and elements to minimise lens aberrations. For modelling purposes the

lens system can be treated as a single diffraction limited lens [23]. Further degradation in the optics MTF may be caused by an anti-aliasing filter, which can be modelled by a birefringent technique [24]. The MTF of the electro-mechanical components of the device is governed by the stepper-driven mechanism. Two general models for MTF degradation due to motion may be combined to account for their effects. The first is the linear motion MTF, affecting the frequency response of the system in the direction of the motion [23]. The second, representing degradation due to random jitter, is the random motion MTF, described by a Gaussian function having a standard deviation equal to the rms random displacement [25].

Because the MTF depends critically on the method of measurement due to non-linearities the system introduces, the overall MTF of the scanner has been determined using three different techniques which gave different results [26]. Figure 6 presents MTFs for the fast (electronic scan along the CCD array) and the slow (in the direction of mechanical transport) scanning directions, evaluated using the ISO 12233 Slanted Edge SFR plug-in [27]. The curves represent the monochrome frequency responses of the centre of the scanning frame and at the optical resolution of the device. The ISO 12233 Slanted Edge SFR plug-in (for Adobe Photoshop software) was originally developed to determine the SFR of digital cameras from images of sloping edges. It generates one-dimensional uniformly super-sampled edge profiles, which are used to calculate the average spatial frequency response of the system. This method, introduced by Reichenbach *et al.* [28], is based on the traditional edge technique but explicitly deals with fundamental sampled system considerations. Note that, although the term SFR is used in place of MTF in the official title of the plug-in to avoid confusion with photographic MTF [29], here we refer to the result yielded from the plug-in calculations as SFR and to that corrected for the frequency content of the test target as MTF.

Custom-made test-targets were created from quality laser printed edges, recorded at a magnification 0.19 on Ilford Pan-F Plus professional black-and-white film, at various angles ranging between 13° and 16° from the vertical [26,30]. A 10-step Kodak neutral grey scale was photographed together with the edge for the evaluation the opto-electronic conversion function (OECF). An example of a test-target is illustrated in Figure 7. The density difference of the recorded edge on the film was 0.80, with the light part of the edge having density equal to 0.40 and the dark part 1.20. The frequency content of the edge-target (shown in Figure 8 until just above the Nyquist frequency of the scanner) was evaluated using the traditional edge technique [31] and a calibrated Joyce Loebel 3CS microdensitometer. Scanning was performed with the edge falling first horizontally and then vertically with respect to the scanning frame, to evaluate the SFR for the fast and slow scanning directions. Several scans were performed, by translating slightly the edge and average responses were calculated for the central scanning

area. Figure 6 shows that the extracted MTFs are similar for both scanning directions, with the slow scan having a slightly lower response at frequencies beyond 15 cycles/mm, an area more prone to experimental inaccuracies. Since the sampling aperture of such devices is most often square [23,32] the isotropic scanner response at 90° orientation is an expected result.

### 3.3 Spatial uniformity

Various parameters affect the spatial uniformity of the scanner, such as LED and electrical inconsistencies, CCD spatial variations, stepper-driven stage speed variations, and others. The spatial uniformity of the system was assessed in density units, by employing a Kodak uniformity target<sup>3</sup> [33] of average density 1.70. Uniformity profiles around zero mean density for the monochrome and the colour channels of the scanner are presented in Figures 9 and 10 respectively, indicating non-uniformity within the scanning area of magnitude up to 0.05 density units for monochrome scans and up to 0.10 units for colour scans. A correction factor for each pixel location in the acquired image could be built to accommodate the scanning non-uniformity. This task was not carried out because it can produce contouring artefacts due to quantization errors in the 24-bit output space of the device. Additionally, information on the error at different levels of scanner's response would be necessary to build a complete correction model dealing with real, tonally complex images.

### 3.4 Colour characterisation

Device independent colour requires a colorimetric scanner. The Nikon LS-1000 scanner, like most commercial scanners, is not colorimetric. In order for a scanner to have colorimetric properties, the spectral response functions should be equal to the CIE colour matching functions (the Luther condition) or a linear combination of them. Although the design of colorimetric scanners has been explored [34,35], in practice it is difficult to achieve because colorimetric scanning requires sufficient quantization levels, a very large dynamic range, high signal to noise ratio and narrow band filters [36]. Various workers have proposed methods to produce colorimetric values from non-colorimetric scanners over the last decade. These include: the use of polynomial regression to derive a colour correction matrix [37-39], the creation of LUTs by interpolation between measured points [40-41], dye concentration modelling [36,42,43] and neural networks [44,45]. Effort has also been put into developing techniques for converting colour scanners into colorimeters [46]. Colorimetric characterisation of the Nikon LS-1000 scanner was carried out using polynomial regression to relate scanner RGB to CIEXYZ values. The choice of method was based on availability of

---

<sup>3</sup> The target was kindly lent for this project by the Eastman Kodak research laboratories in Rochester.

measuring equipment and targets in our laboratory, on its simplicity and wide use (i.e. well known and documented) and its degree of success in characterising non-colorimetric imaging devices. The transformation from RGB to CIEXYZ forms the first step in developing a device-independent description of colour in non-colorimetric devices [47]. From CIEXYZ direct transformation to many rendered and all CIE colour spaces is possible.

The characterisation of the scanner consisted of two steps. First, the grey-balance of the red, green and blue signals, obtained by setting  $R=G=B=f(Y)$  for the neutral patches of the calibration target, where  $f(Y)$  is a function of luminance,  $Y$ . In this application, the luminance itself was used for the linearization of the signals. Secondly, the derivation of a  $3 \times m$  colour correction matrix used for colour transformation was determined. The matrix was derived through the use of polynomial regressions to selected samples with known colour specifications in both source (CIEXYZ) and destination (grey-balanced RGB) colour systems. The polynomial regression is based on the assumption that the correlation between source and destination colour system can be approximated by a set of simultaneous equations. The grey balanced R,G, and B data are the independent variables, the X, Y, and Z tristimulus values are the dependent variables and the correction matrix is the set of coefficients.

The polynomial regression method for device characterisation is constrained to a single set of dyes, illuminant and observer and ignores the problem of metamerism. Since the RPS collection of slides was on Ektachrome material, the Kodak Q-60E3 test target on Ektachrome transparency film was selected to best characterise the scanner. The target fulfils the requirements of a test object for an input colour scanner [48], providing uniform mapping in the CIELAB colour space. All the 264 patches of the Q-60E3 were used as the training set of samples. This decision was based on the argument that samples that are not used in the regression may still have considerable colorimetric errors. The target illuminant and observer conditions were the CIE illuminant  $D_{65}$  and the CIE 1931 2° Standard Colorimetric Observer respectively. Since the primary output of the digital image archive was a CRT display system, little adjustment is required on a typical monitor to achieve a white point with correlated colour temperature close to 6500K. Finally,  $D_{65}$  is the reference display white point of the Standard RGB (sRGB) colour space, which was the output colour space of the digital archive (see Section 4).

The performance of various degrees of polynomials was assessed, with the number of coefficients,  $m$ , ranging from 6 to 31. Colour differences between original and calculated colours were determined in CIELAB space, since any other direct measure of the polynomial fit between RGB and XYZ (such as the correlation coefficient for example) does not correlate

with human visual performance. The CIE  $\Delta E^*_{94}$  colour difference formula [49] could be used instead of CIE  $\Delta E^*_{ab}$  in the colorimetric analysis, which corrects for a significant uniformity error of the  $\Delta E^*_{ab}$ , in that colour pairs of high chroma produce larger numerical differences than their appearance justifies. However, the choice of formula was dictated by familiarity and common practice.  $\Delta E^*_{94}$  has been designed and, until now, has been mostly used in graphic arts applications to evaluate differences in uniform reflection samples. The individual parametric factors in  $\Delta E^*_{94}$  formula are not fixed outside the reference conditions (as CRT conditions and pictorial scenes that this project is concerned with). Also, the perceptibility and acceptability of  $\Delta E^*_{94}$  differences have not been yet well established or widely used for display conditions and pictorial images, contrary to the CIE  $\Delta E^*_{ab}$  differences.

All calculations were performed in MATLAB software, where appropriate functions were built for the calibration of the scanned archive. Table 3 presents average and maximum colour differences,  $\Delta E^*_{ab}$ , together with the percentage of samples having a  $\Delta E^*_{ab}$  up to 2.5 units, for each correction matrix. The value of  $\Delta E^*_{ab}$  2.5 was chosen as an aim point because it has been demonstrated to be the limit of perceptibility tolerance in complex scenes, displayed on common CRTs [50]. Figure 11 illustrates the distribution of  $\Delta E^*_{ab}$  for the three most successful colour matrices. The colorimetric performance of the correction matrices improved, as expected, with increasing number of polynomial terms. Since gamut compression is inevitable, perfect colour matches cannot be achieved. This was noticed in large colorimetric errors of specific patches, which only decreased partially by increasing the number of polynomial terms. The overall results are not very encouraging, until the 3 x 31 matrix, where the average  $\Delta E^*_{ab}$  is 2.12 and 76% of the samples have  $\Delta E^*_{ab}$  below 2.5. The problem, however, with the polynomial regression is that using high order transformation equations can lead to poor performance in practice. This is a result of fitting random error in addition to the desired systematic trends and noise amplification [36].

A comparison between the original and estimated CIE  $a^*$  and  $b^*$  chromaticities of all the samples of the Q-60E3 target is shown in Figure 12 for the 3 x 31 matrix. Greatest discrepancies can be seen in the yellow-green and blue-red quadrants, and in the outer regions of the chromaticity diagram. Less significant differences are reasonably random. The average and maximum  $\Delta L^*$ ,  $\Delta C^*_{ab}$  and  $\Delta H^*_{ab}$  were found 0.28, 1.46 and 1.25 and 2.18, 14.21 and 10.62 respectively. These values indicate that colorimetric differences occurred mostly due to chroma and then to hue shifts. A plot of  $\Delta E^*_{ab}$  versus original colour lightness, in Figure 13, indicates increased error mostly in the darker colours.

A severe limitation of this transformation was the loss of grey balance. Figure 14 presents the colorimetric errors for the 24-step greyscale of the target, where it appears that important chroma and hue errors resulted to  $\Delta E^*_{ab}$  values up to 8.15. The figure indicates that while the white point was retained, colour differences beyond  $2.5 \Delta E^*_{ab}$  were found for the darker steps of the greyscale (from step 16 to 24). It was observed that in both colour and neutral patches, chroma and hue shifts contributed largely to the high colorimetric differences, whereas lightness errors were small. Nonetheless, hue and chroma errors can be considered as visually less significant when they occur in darker areas [14], especially when images are displayed on CRTs which have medium-to-low brightness and finite contrast ratios. The loss of grey balance was not corrected manually.

Colorimetric errors in this application were always calculated from the training set of colours. In practice, it is known that when reproducing colours other than the training colours (i.e. testing colours) the error increases due to colours not being taken into account in the regression [38,39]. With the  $3 \times 31$  matrix and the 264 training colours employed here, the error in the testing colours should not exceed 3.0 to  $3.2 \Delta E^*_{ab}$ . This estimation is based in data provided by Kang, who produced a table of errors for both training and testing colours for a given media and various matrix sizes [51].

A comparison of the colour gamut of the scanner primaries (when scanning Ektachrome) and the sRGB colour space, plot on the 1976 CIE  $u'v'$  diagram, is given in Figure 15. The gamuts presented here are the maximum gamuts attainable by each device. They appear somewhat shifted in position. It is noticed that the green primaries are similar whereas the red and the blue primaries differ, with the scanner red being purer than the sRGB red and the sRGB blue being purer than the scanner blue.

The RPS slides were scanned in the same fashion as the Q-60E3 target and converted to colorimetric digital files using the  $3 \times 31$  colour correction matrix.

#### **4. Image encoding for display output**

Direct access to the digital images via most commercially available imaging applications and systems was achieved by encoding the image data from the 1931 CIE XYZ  $D_{65}$  system to the Standard RGB (sRGB) [52] colour space. The sRGB colour space is an interchange RGB colour space, calibrated colorimetrically for a reference display output, default viewing conditions and a reference observer. The reference display consists of a CRT coated with an IUT-R 709.BT set of phosphors, employed in the High Definition Television (HDTV). The

reference display gamma is set to 2.2 and it is assumed to be the gamma of a correctly adjusted CRT with no additional gamma correction imposed by the frame buffer. The reference viewing conditions involve dim ambient illumination (64 lux), with chromaticities of the white point those of CIE D<sub>50</sub>, and relatively low veiling glare (1%). The sRGB colour encoding provides standard compatibility with various large image collections. These include the collection of the National Geographic Society, USA, the US Library of Congress and most collections based on television capture [53].

The encoding from CIEXYZ to sRGB digital counts involves a linear transformation, to convert the CIEXYZ values to linear normalised RGB values. The appropriate gamma-correction function, with an exponent of 1/2.4 and an offset of 0.055, is applied to the RGB values to compensate for a display with the simple exponent value of 2.2. The resulting numbers are scaled to produce 8 bit per channel digital counts. The inverse transformation can be applied to recover the original CIEXYZ values. Original tristimulus values outside the sRGB gamut cannot, however, be recovered unless they are saved independently to be used for the necessary calculations. In the RGB encoding process, negative values and values greater than 1.0 are not retained. In such cases the RGB values are limited between 0 and 1.0 by clipping. The clipped values, which indicate colours out of the sRGB gamut, are shown for the Q-60E3 test target in Figure 16. The figure presents the red, green and blue planes of the image, where the error is indicated in white and the values inside the sRGB gamut in black. The percentages of the clipped values for the red, green and blue channels were 5.0%, 1.4% and 2.5% respectively. Clipping occurred mostly in darker orange-yellow, green and cyan colours (with lightness between 15% and 30%) and in highly chromatic cyan and yellow colours. Image artefacts (such as contouring for example) were not noticed when the images were inspected on a sRGB-compatible display. A general observation concerning the original photographs is that, in total, they are low chroma, low contrast images [14]. Therefore, the direct consequences of the sRGB gamut limitations to the scanned archive should not be as significant as they are for the Q-60 target, employed for the sRGB evaluation.

Digital image files encoded in sRGB are delivered to the user while retaining their appearance only under the reference sRGB display and viewing conditions. Modern CRTs have common (or closely related) primaries and tonal characteristics and can be calibrated to match the reference display using fairly inexpensive apparatus. Consistent viewing conditions are nevertheless more difficult to achieve. Variations in the colour of the illuminance from the reference illuminance would cause a shift on the perceived white point, since when viewing images on a CRT under certain conditions the state of adaptation is affected by both the monitor white point and the room illumination [54]. The extent of the chromatic adaptation

will be reduced at reduced display luminance and at increased differences in illuminance chromaticity [55]. Variations in the levels of illuminance will cause a shift mainly in the perceived image contrast, but also perceived colour saturation. At darker than the reference surrounds the sRGB images will appear with reduced contrast, since the effect of the dark surround is to make the display elements brighter, but to a greater extent for dark areas. At lighter than the reference surrounds (such as in typical office conditions [52]) the opposite effect takes place, but it is somehow compensated for by the increased veiling glare, which reduces more the darkness of the blacks. For viewing conditions that are not compliant with the reference conditions, the CIECAM97 colour appearance model is recommended for the appropriate transformations, along with some additional calculations for veiling glare and black mapping compensation [52].

An ICC (International Color Consortium) sRGB profile [56] was provided along with the digital images, for use when the images are reproduced in a system other than a CRT. ICC colour profiles are supported by most current operating systems, image manipulation and desktop publishing applications. Theoretically, the input ICC profile provides the user of the archive with an additional tool for correct colour imaging, on condition that the ICC profile of the output device, including the viewing conditions, is on hand. In practice, the use of the ICC profiles does not guarantee consistent colour imaging, primarily because the Profile Colour Space (PCS) does not adequately define various aspects of the reference space, such as flare, white and black points [57]. Additionally, images processed by different engines may produce significant colour differences due to the varying strategies for gamut mapping.

## **5. Storage and data migration**

International storage standards were used in this project to provide easy access while enabling the digital files and storage media to be successfully transferred to future media and formats. The processed images comprising the archive were saved as sRGB, TIFF (Tagged Image Format) files and were stored on an ISO 9660 format writable compact disks (CD-Rs), each holding 640 MB of data. TIFF is thoroughly documented and the source code is available. It is supported by all computer platforms and by the majority of imaging applications and desktop publishing software. Easy access and retrieval makes TIFF the most advisable image file format for image archiving purposes [58]. The ISO CD-ROM recording format also allows access to the data from all current platforms and operating systems.

Longevity in all storage media depends on the stability of the medium, the storage conditions and handling [59]. CD-ROM degradation can be caused by oxidation and structural changes

and therefore storage temperature and humidity are determinants of the useful lifetime of the disks. Optical media manufacturers, using data from various accelerated ageing experiments, claim estimated physical lifetime for CD-ROMs of approximately 100 years, but without handling, and give a guarantee of 25 to 30 years [60,61]. Storage temperatures and storage humidity suggested by the ISO 9660 standard are nowadays considered too high. The recommended environmental conditions are 23° C and relative humidity between 20% and 50%, where the lower levels provide increased stability [59]. Temperature and relative humidity fluctuations may damage CD-ROMs even more rapidly but, unlike magnetic media, magnetic fields do not have any effect on them.

Along with the relatively long physical lifetime and high data capacity, there are other attributes, which make the CD-ROM the most appropriate medium for image distribution and storage purposes. Fast random access of large files is achieved because of the continuous sequence of sectors on the spiral layout of the disk. CD-ROMs are removable media, which can be duplicated very easily. They have a write-once capability, which provides high security from data erasure or modification with frequent access to the records. The media price per MB, when bought in relatively large quantities, is currently below the cost of any other random access memory. Finally the CD-ROM manufacture, disk players and software retrieval conform to industry and international standards.

Unfortunately, it is impossible to rely on the hardware and software (H/S) used to read, write and store the digital images being available in the future. Although there have been suggestions for developing a standard H/S configuration that all future magnetic or optical products must adhere to, in practice this would inhibit the development of new technologies [59]. Therefore, preservation of information on optical disks means transferring from obsolete to newer systems, i.e. data migration. There is no degradation in the digital migration process. Provided that migration periods are well defined and the refreshing of information is performed regularly, the digital archive should have long life-expectancy.

Obsolescence of the file format and future compatibility of the colour encoding are of principal consideration. In many cases, it is suggested that the refreshing of information is effective as a preservation technique only as long as the information is encoded in a format which is independent of a particular hardware or software, such as ascii [61,62]. Although this might be a gateway in preservation issues it is an impractical solution since it makes the direct access to the digital images impossible. Thus, the support of the TIFF is the major concern governing the migration periods of the digital archive. The first version of the TIFF was published in 1986 and since the structure of TIFF has been expanded around a basic frame,

which makes the older versions backwards compatible. The TIFF 6 revision was released in 1992 [63].

The sRGB is a well-defined standard RGB colour space, well-suited for the CRT-based workflow. Because it has been widely adopted it is expected by its developers and supporters to remain popular in the years to come [64]. The life-span of the sRGB encoding may however be shorter than anticipated due to the rapid evolution of the display technology. Only a few years ago, the CRT was thought to remain the predominant display technology in the future [65]. Today, while CRTs are still improving, new display technologies (such as TFT-based flat panel and plasma displays) are also growing rapidly. In such displays, the colour primaries, transfer characteristics, dynamic range and viewing conditions differ than those of CRTs [66], resulting to poor tone and colour accuracy. The sRGB ICC profile provided with the digital images can help the communication of colour in alternative systems and viewing conditions. The future of ICC profiles is nevertheless not guaranteed. Currently, various users refuse to incorporate them in their files. Reversing from sRGB to original linear XYZ data and re-optimising for a difference display could be worth, only if the image bit-depth was higher and the colour gamut was not restricted.

Obsolescence of the H/S used to read the optical disk is a second issue. Associated H/S includes the CD-ROM reader, the software driving the reader (driver), the host computer and its operating system. Hardware becomes obsolete in relatively short periods; a new generation is expected approximately every two years. Generally, a new generation of hardware is backwards compatible for two generations [58]. Driving software usually changes with or within the lifetime of the device (hardware) to be compatible with newer operating systems, providing new features for the user. A given device can be operated by four successive generations of drivers. Operating systems are renewed every one to three years, but usually run drivers written for the previous two versions. In total, although optical disks have a relatively long physical lifetime, the estimated time of obsolescence of a particular recording due to hardware and software configurations is estimated between five to eight years [61,67].

Eventually, the physical media supporting the digital image archive will become obsolete. The Digital Versatile Disk (DVD), of the same physical size as the CD-ROM (120mm) but with increased data capacity, appears to be an obvious successor. A considerable advantage for the useful lifetime of the CD-ROM archive as well as for the migration of the data from this media is that several manufacturers currently distribute platforms with DVD-CD-ROM drives. DVD media are being developing assuming the inheritance of existing software resources and will continue to maintain compatibility in the future [68]. Otherwise, annually

storing back-up copies on magnetic tapes is an advisable practice. Magnetic tapes are inexpensive, have large capacity but are of short physical lifetime.

According to some organisations and individuals dealing with the preservation of digital information, the complexities of migration represents a real threat to the life of information [62]. Migration, however, is the only solution to the long-term access of the data and should be considered as a routine task and a recurring cost in operating a digital image archive.

In the present collection, as for many collections, limitations of the input device and the choice of a rendering colour space for image encoding have imposed restricted quality in the digital reproductions. Whether the image data is worth migrating will depend on the current use of the digital archive, i.e. to what extent it is used and how well it satisfies the needs of the users. Also, it will depend on possible future changes in imaging systems, i.e. the available data will be of an insufficient quality when compared with newer systems and standards.

## **6. Summary and Conclusions**

The digitisation of a collection of photographs is a complex operation, involving many decisions, concerning the way the original image is digitally acquired, transformed into a device independent colour space and saved in an appropriate colour space and medium. The choice of equipment and methods are determinants of the quality of the reproduction and it is based primarily on the current and also future uses of the digital collection but also on available budgets, time and manpower. In this project, the primary objective for digitisation was to provide accessibility to a collection which otherwise was closed to viewing.

Digitisation was performed using a commercially available scanner, producing 24-bit colour images of spatial resolution 2800 by 3500 pixels. Characterisation of the device showed that the system imposed quality limitations on the final reproduction. In terms of tones, the dynamic range of the scanner was not capable of covering the entire density range of the original colour reversal material. As a consequence, original tones were compressed or clipped to match the effective range of the device. Additionally, the 8-bit per channel output space of the scanner limited the precision of post-acquisition processes, necessary for image calibration. In sharpness assessments, measurements of the MTF of the scanner indicated similar spatial frequency responses in the two scanning orientations, which fell quickly with increasing frequency. The MTF degradation could be partially compensated after the digital acquisition with the use of digital filters providing image sharpening. Sharpening was not

applied to the images. Some degree of image sharpening can however be achieved by the users of the archive in most rendering applications.

A 3 x 31 colour correction matrix was employed to convert the scanner output values to colorimetric values. The matrix was shown to produce average colorimetric differences within the limit of perceptibility for complex scenes displayed on CRTs. High colorimetric errors were identified mostly in darker patches, in the yellow-green and red-violet regions. The colour transformation resulted in a loss of grey balance, also noticed in the darker neutral patches. It was observed that, in both colour and neutral patches, chroma and hue shifts contributed largely to the high colorimetric differences whereas lightness errors were small. Hue and chroma errors may, nevertheless, be considered as visually less significant when they occur in darker colours, especially when images are displayed on CRTs.

The choice of image encoding of the digital archive to the sRGB colour space was a trade-off between accessibility and losses in the available colour gamut. In this study, it was shown that 9% of the available colours of the scanned Q-60E3 target were out of the sRGB gamut. For communicating the images in other than sRGB compatible media, an sRGB ICC profile was provided together with the digital image archive.

Colorimetric images were stored using a file format and media compatible with the majority of current hardware/software configurations. A requisite for securing the longevity of the digital archive is the migration of the data from the current to newer systems. The migration process is a demanding operation, involving the follow-up of the technologies and has considerable costs. Whether the produced image data is worth migrating will depend on the effective use of the digital archive as well as on future improvement of imaging systems.

### **Acknowledgements**

The authors are indebted to Pamela Roberts of The Royal Photographic Society for provision of the slides used in this project and for helpful discussion and encouragement. We should also like to thank Clare Birdsey of the ITRG for discussion, help and advice in support of the project.

## References

1. **Birdsey, C.L., Golding, A. and Jacobson, R.E.** The suitability of employing digital technology for accessing photographic collections, *Convergence*, 1999, **6**, 123-130.
2. **Keefe, L.E. and Inch, D.** *The Life of a Photograph: Archival Processing, Matting, Framing, Storage*, 1990, 2<sup>nd</sup> edition, Ch. 15, p. 245 (Focal Press, Stoneham).
3. **Gschwind, R. and Frey, F.** Electronic imaging, a tool for the reconstruction of faded color photographs *J. Imaging Sci. Techn.*, 1994, **38**, 520-525.
4. **Saunders, D.** High quality imaging at the National Gallery *Comput. Humanities*, 1997, **31**, 153-167.
5. **Martinez, K., Cupitt, J. and Saunders, D** In *Proc. SPIE*, p. 25 (1993).
6. **Süsstrunk, S.** In *Proc. ICPS*, Antwerp, **2**, p. 232 (1998).
7. **Frey, F. and Süsstrunk, S.** In *Proc. SPIE*, p. 2 (1996).
8. **Frey, F.** In *Proc. ICPS*, Antwerp, **2**, p. 228 (1998).
9. **Frey, F.** In *Proc. SPIE*, p. 49 (1997).
10. **Miyake, Y., Inoue, S., Tamoto, Y. and Kubo, S.** In *Proc. RPS Photographic and Electronic Image Quality*, Bath (1984).
11. **Birdsey, C.L.** *Design, production and implementation of a digitised photographic archive*, MPhil to PhD transfer report, 1998 (University of Westminster, London).
12. **Honjo, S. and Kriss, M.A.** In *Handbook of Photographic Science and Engineering*, (Ed. C.N. Proudfoot), 1996 (IS&T, USA).
13. Nikon LS-1000 35 mm Desktop Film Scanner, device specifications, Nikon Corporation, technical sheet no. 6CE51801 (9509-04)K, Japan (1995).
14. **Triantaphillidou, S.** *Aspects of image quality for the digitisation of photographic collections*, PhD thesis, 2001, (University of Westminster, London).
15. **Dainty, J.C. and Shaw, R.** *Image Science: Principles, Analysis and Evaluation of Photographic-Type Processes*, 1974, Ch. 6, p. 190 (Academic Press, London).
16. Kodak Ektachrome 100 Plus Professional Film, Kodak publication No E-113 CAT 122 0443 (1997).
17. **Lehmbeck, D.R. and Urbach, J.C.** In *Optical Scanning* (Ed. G.F. Marshall), 1991, Ch. 3, p. 83 (Marcel Dekker, New York).
18. **Eliezer, C.** Leaf HDR: Remaking the color high end on the desktop *The Seybold Report on Desktop Publishing*, 1993, **7**, 3-10.
19. **Poynton, C.A.** “gamma” and its disguises: The non-linear mapping of intensity in perception, CRTs, film and video. *J. SMPTE*, 1993, **102**, 1099-1108.
20. **Triantaphillidou, S., Jacobson, R.E. and Ford, A.M.** In . In *Proc. ICPS*, Antwerp, **2**, p. 204 (1998).

21. ISO 16067-1 Photography – Electronic scanners for photographic images – Spatial resolution measurements – Part 1: scanners for reflective media. Available at: [http://www.pima.net/standards/iso/tc42/wg18\\_POW.htm](http://www.pima.net/standards/iso/tc42/wg18_POW.htm) (2001).
22. **MacDonald, L.W.** Tone and quality issues in digital cameras *J. Photogr. Sci.*, 1996, **44**, 18-20.
23. **Holst, G.C.** *CCD Arrays Cameras and Displays*, 1996, Ch. 10, p.233, (SPIE Optical Engineering Press, USA).
24. **Kriss, M.A.** In *Proc. SPIE, Can-Am*, p. 4 (1990).
25. **Shea, J.J.** ‘Lunar limb knife-edge optical transfer function measurements *J. Electron. Imaging*, 1999, **8**, 196-208.
26. **Triantaphillidou, S., Jacobson, R.E. and Fagard-Jenkin, R.** In *Proc. IS&T PICS*, Savanna, p. 231 (1999).
27. ISO 12233:2000, Photography – Electronic picture camera – Resolution measurements. International Standard Organisation (2000).
28. **Reichenbach, S.E., Park, S.K. and Narayanswamy, R.** Characterising digital image acquisition devices *Opt. Eng.*, 1991, **30**, 170-177.
29. ANSI PH 2.39-1977 (R1990). Method of measuring the photographic modulation transfer function of continuous-tone, black-and-white photographic films (1997).
30. **Williams, D.** In *Proc. IS&T PICS*, Portland, p. 133 (1998).
31. **Jones, R.A.** An automatic technique for deriving MTFs from edge traces *Photogr. Sci. Eng.*, 1967, **11**, 102-106.
32. **Theuwissen, A.J.P.** *Solid-State Imaging with Charge-Coupled Devices*, 1995, Ch. 4, p. 113 (Kluwer Academic Publishers, Mashahushetts).
33. **Ptucha, R.W.** In *Proc. IS&T PICS*, Savanna, p. 125 (1999).
34. **Engeldrum, P.G.** In *Proc. SPIE*, p. 75 (1993).
35. **Vrhel, M.J. and Trussell, H.J.** Filter considerations in color correction, *IEEE T. Image Process.*, 1994, **3**, 147-161.
36. **Berns, R.S. and Shyu, M.J.** Colorimetric characterization of a desktop scanner using a spectral model, *J. Electron. Imaging*, 1995, **4**, 360-372.
37. **Hung, P.C.** In *Proc. SPIE*, p. 164 (1991).
38. **Kang, H.R.** Color space calibration, *J. Imaging Sci. Techn.*, 1992, **36**, 162-170.
39. **Clippeeler, J.D.** In *Proc. TAGA*, p. 98 (1993).
40. **Hung, P.C.** Colorimetric calibration in electronic imaging devices using a look-up-table model and interpolations, *J. Electron. Imaging*, 1993, **2**, 53-61.
41. **Kasson, J.M., Plouffe, W., and Nin S.I.** In *Proc. SPIE*, p. 127 (1993).
42. **Rodriguez, M.A. and Stockham, T.G.** In *Proc. SPIE*, p. 413 (1993).

43. **Jung, N. and Tralle, C.** An alternative method of optoelectronic color analysis for slides *Signal Process.-Image*, 1992, **6**, 47-57.
44. **Kang, H.R. and Anderson, P.G.** Neural network application to the color scanner and printer calibration, *J. Electron. Imaging*, 1992, **1**, 25-135.
45. **Schettini, R., Barolo, B. and Boldrin, E.** Colorimetric calibration of color scanners by back-propagation, *Pattern Recogn. Lett.*, 1992, **16**, 1051-1056
46. **Farrell, J., Sherman, D. and Wandell, B.A.** In *Proc. IS&T Tenth International Congress on Advances in Non-Impact Printing Technologies*, p. 579 (1994).
47. **Wandell, B.A. and Farrell, J.E.** In *Proc. SPIE*, p. 92 (1993).
48. **Maier, T.O. and Rinehart, C.E.** Design criteria for an input colour scanner evaluation test object *J. Photogr. Sci.*, 1990, 169-172.
49. Industrial Colour-Difference Evaluation, CIE Technical Report 116-1995, Vienna, (1995).
50. **Stokes, M., Fairchild, M.D. and Berns, R.S.** Precision requirements for digital color reproduction *ACM T. Graphic.*, 1992, **11**, 406-422.
51. **Kang, H.R.**, *Color Technology for Electronic Imaging Devices*, 1997, Ch. 11, p.288, (SPIE Optical Engineering Press, USA).
52. IEC 61966-2-1: Multimedia systems and equipment – Colour measurement and management – Part 2-1: Colour management – Default RGB colour space –sRGB (1999).
53. **Stokes, M. Nielsen, M. and Zimmerman, D.** What is sRGB, Internet publication: <http://www.srgb.com/sRGBOverview> (1998).
54. **Katoh, N., Nakabayashi, K., Ito, M. and Ohno, S.** Effect of ambient light on the color appearance of softcopy images: Mixed chromatic adaptation for self-luminous displays *J. Electron. Imaging*, 1998, **7**, 794-806.
55. **Hunt, R.W.** Viewing parameters affecting self-luminous, reflection and transmissive colours *Displays*, 1996, **4**, 157-162.
56. sRGB ICC Profile, Available at: <http://www.srgb.com/sRGBICCProfile.html> (1999).
57. **MacDonald, L.W.** Developments in colour management systems *Displays*, 1996, **16**, 203-211.
58. **Rosenthaler, L. and Gschwind, R** In *Proc. ICPS*, Antwerp, **2**, p. 239 (1998).
59. **Adelstein, P.Z. and Frey, F.** In *Proc. IS&T PICS*, Portland, p. 127 (1998).
60. **Arps, A.** In *Preservation of electronic formats & electronic formats for preservation* (Ed. J.Mohlhenrich), 1993, Ch. 5, p. 83 (Highsmith Press, Winconsin).
61. **Rothenberg, J.** Ensuring the longevity of digital documents *Sci. Am.*, 1995, Jan., 24-29.
62. The Commission on Preservation and Access and the Research Library Group, ‘Preserving digital information’, Report for the task of archiving of digital information, USA (1996).

63. Adobe Developers Association, 'TIFF revision 6.0', Internet publication:  
<http://www.adobe.com/Support/TechNotes.html> (1992).
64. **Gondeck, J.** e-sRGB: An extended sRGB Space for High Quality Consumer Imaging, Revision 2.0. Internet Publication: <http://www.srgb.com/srgb64/PIMA7667-2001.pdf> (2000).
65. **Vandenberghe, P.** In *Proc. ICPS*, Antwerp, **2**, p. 239 (1998).
66. **Süsstrunk, S., Buckley, R. and Swen, S.** In *Proc. IS&T/SID*, p. 127 (1999).
67. **Frey, F. and Süsstrunk, S.** In *proceeding of IEEE ISCAS*, Geneva, p. V-113 (2000).
68. **Yamamoto, M.** Trends in standardization of optical disks *NTT Review*, 1998, **10**, 151-153.

**Table 1:** Effective gamma values and correlation coefficients obtained by linear regression on the normalised logarithmic data for the three scanner channels, for two different targets scanned with *gamma setting* =1.

Channel	$\gamma_s(\text{Q-60E3})$	$r(\text{Q-60E3})$	$\gamma_s(\text{Scala})$	$r(\text{Scala})$
Red	0.95	0.9994	1.26	0.9985
Green	1.06	0.9990	1.22	0.9980
Blue	0.95	0.9997	1.25	0.9966

**Table 2:** Effective gamma values and correlation coefficients obtained by linear regression and calculated gamma values for five different scanner *gamma settings*. Input target: Q-60E3.

Scanner <i>gamma</i>	Effective $\gamma_s$	$r$	Calculated $\gamma_s$	Error
1.00	1.02	0.9999	1.00	+0.02
1.50	0.68	0.9995	0.67	-0.01
2.00	0.51	0.9995	0.50	+0.01
2.50	0.41	0.9994	0.40	+0.01
3.00	0.33	0.9994	0.33	0.00

**Table 3:** Average and maximum  $\Delta E^*_{ab}$  of all samples of the Q-60E3, for 6 correction matrices (3 x *m*).

<i>m</i>	Average $\Delta E^*_{ab}$	Maximum $\Delta E^*_{ab}$	$\Delta E^*_{ab} \leq 2.5$ (%)
6	7.37	69.73	35.2
10	4.80	51.13	40.5
13	4.49	43.45	43.6
19	2.84	21.14	62.6
31	2.12	14.69	76.8

## CAPTIONS TO FIGURES

**Figure 1:** Stages in the production of a collection of digital images.

**Figure 2:** Scanner RGB and monochrome transfer functions plotted in  $\log_{10}$ - $\log_{10}$  space for input target Kodak Q-60E3 on Kodak Ektachrome film.

**Figure 3:** Scanner RGB and monochrome transfer functions plot in  $\log_{10}$ - $\log_{10}$  space for input target produced on Agfa Scala film.

**Figure 4:** Scanner RGB transfer functions plotted according to ISO 16067-1 for input target Kodak Q-60E3 on Kodak Ektachrome film.

**Figure 5:** Monochrome scanner transfer function for five different gamma settings for input target Kodak Q-60E3 on Kodak Ektachrome film.

**Figure 6:** MTFs for the fast and slow scanning directions measured with the Sloping Edge ISO 12233 plug-in.

**Figure 7:** Sloping edge custom-made test-target used for the evaluation of the scanner MTF.

**Figure 8:** Frequency content of the edge target, estimated up to the Nyquist limit of the scanner.

**Figure 9:** Uniformity contour plot, in density units, for the monochrome channel of the scanner.

**Figure 10:** Uniformity contour plots, in density units, for the red (top), green (middle) and blue (bottom) channels of the scanner.

**Figure 11:** Distribution of  $\Delta E^*_{ab}$  between original and estimated CIELAB values for the 3 x 13, 3 x 19 and 3 x 31 correction matrices.

**Figure 12:** Comparison between original (open diamonds) and estimated (solid diamonds) CIE  $a^*$   $b^*$  chromaticities, using the 3 x 31 matrix, for all samples of the Kodak Q-60E3 test target.

**Figure 13:**  $\Delta E^*_{ab}$  versus  $L^*$  for all the colours, using the 3 x 31 matrix.

**Figure 14:** Distribution of  $\Delta E^*_{ab}$ ,  $\Delta L^*$ ,  $\Delta C^*_{ab}$  and  $\Delta H^*_{ab}$  for the neutral patches, when using the 3 x 31 correction matrix.

**Figure 15:** Colour gamuts of the scanner primaries and the sRGB encoding system.

**Figure 16:** Colours of the Kodak Q-60E3 test target which were found out of the sRGB gamut.

Figures

Fig 1.

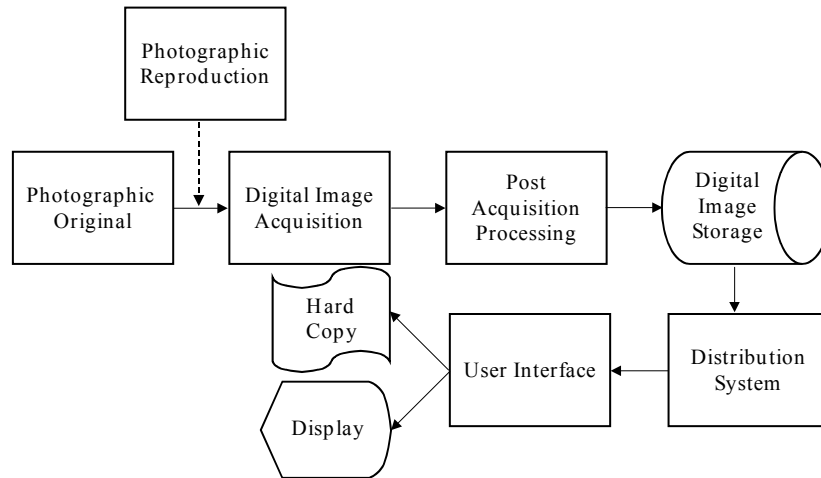


Fig 2.

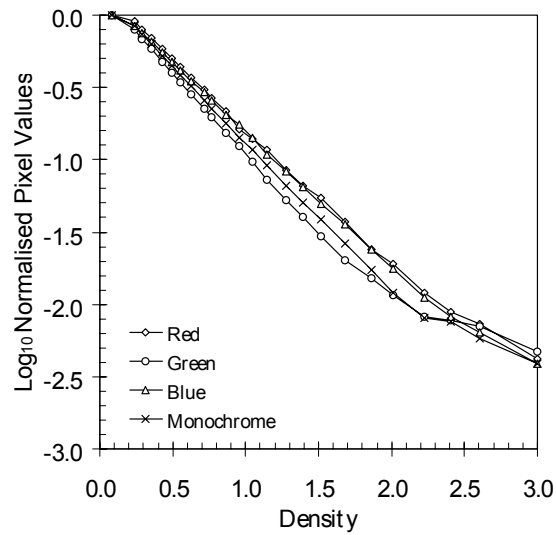


Fig 3.

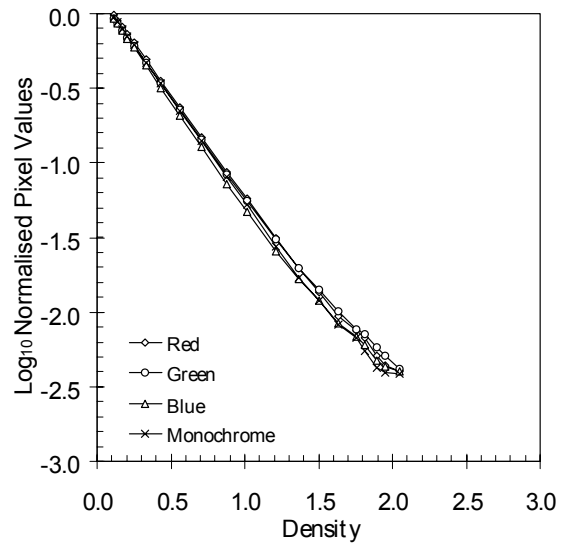


Fig 4.

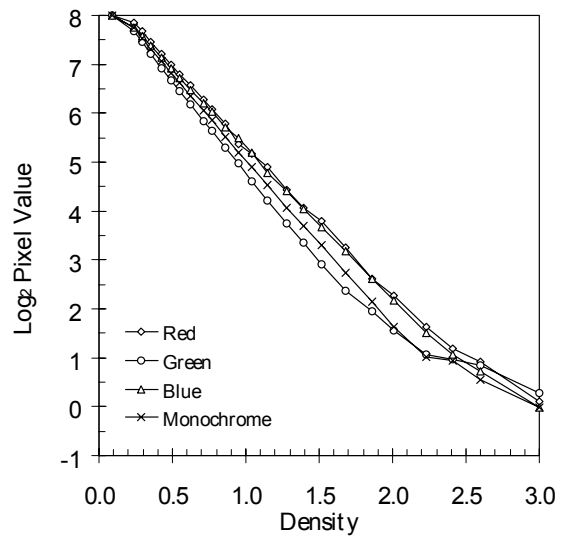


Fig 5.

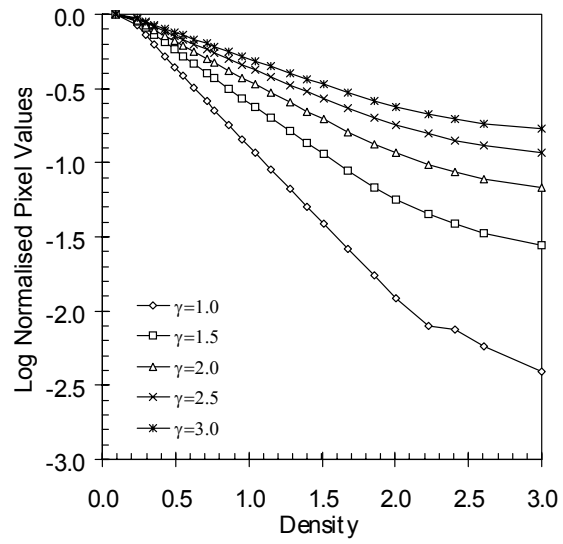


Fig 6.

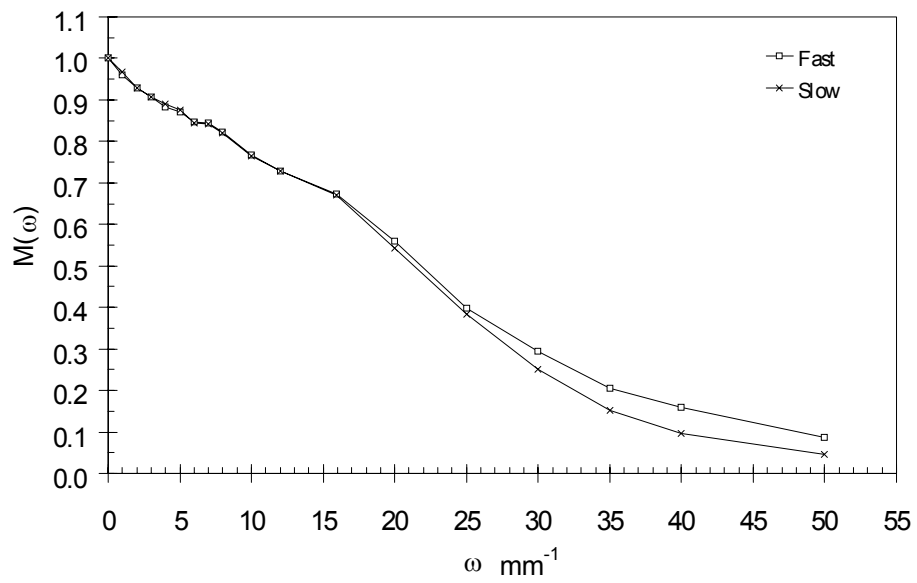


Fig 7.

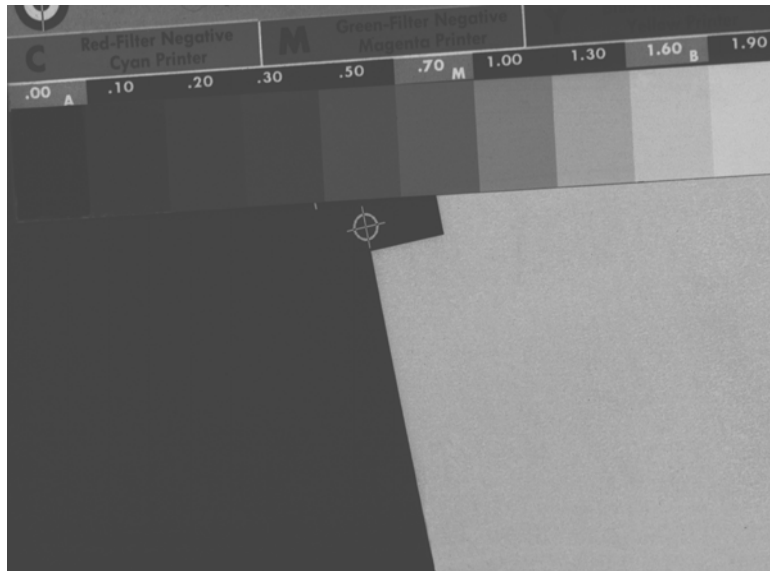


Fig 8.

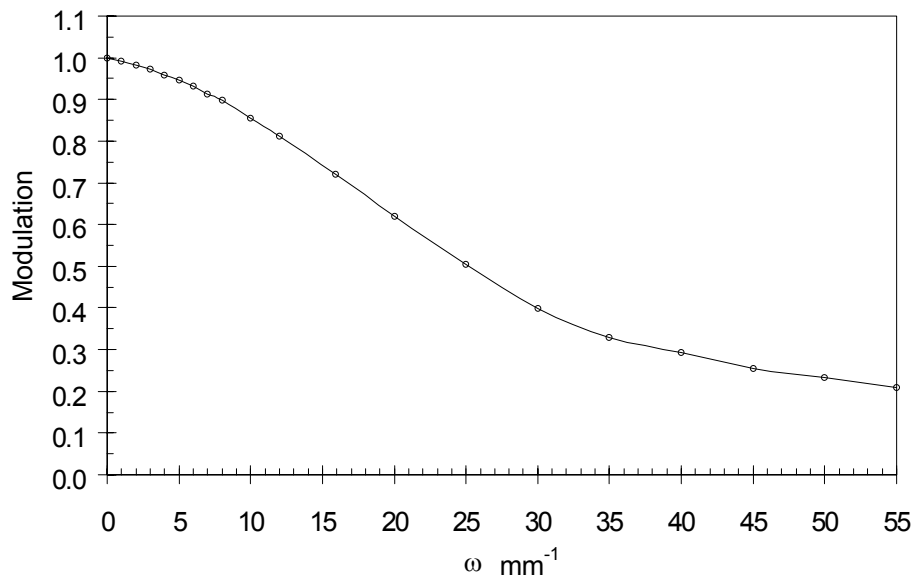


Fig 9.

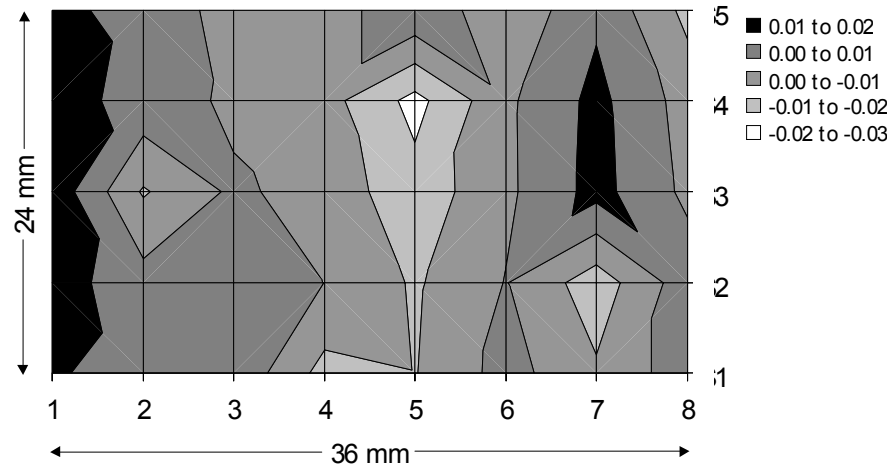


Fig 10.

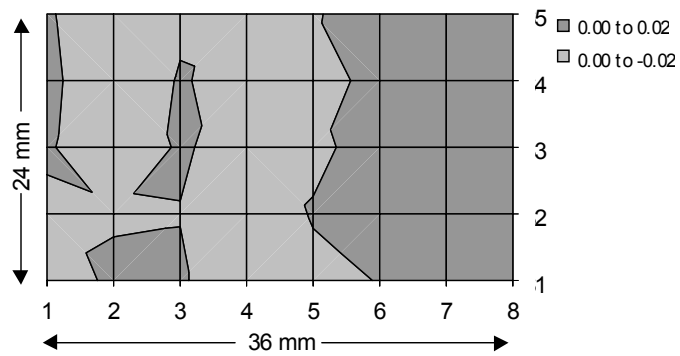
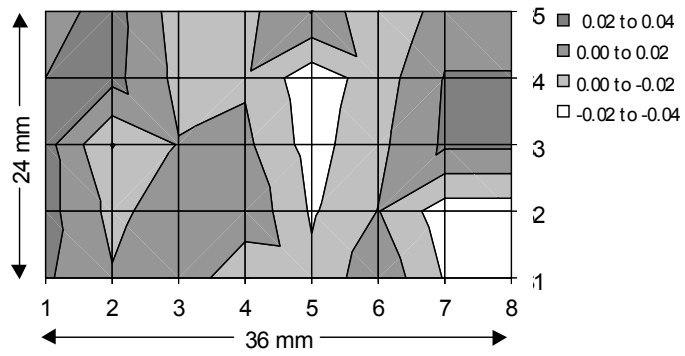
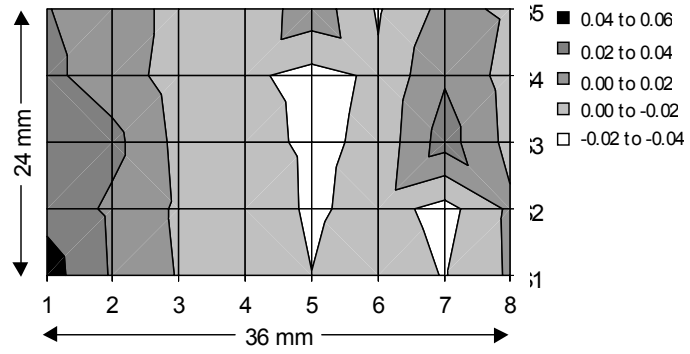


Fig 11.

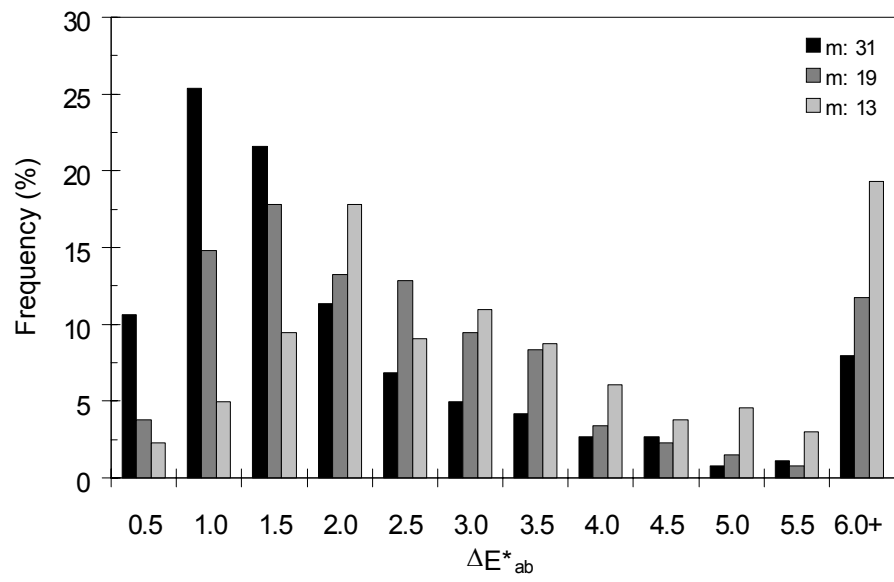


Fig 12.

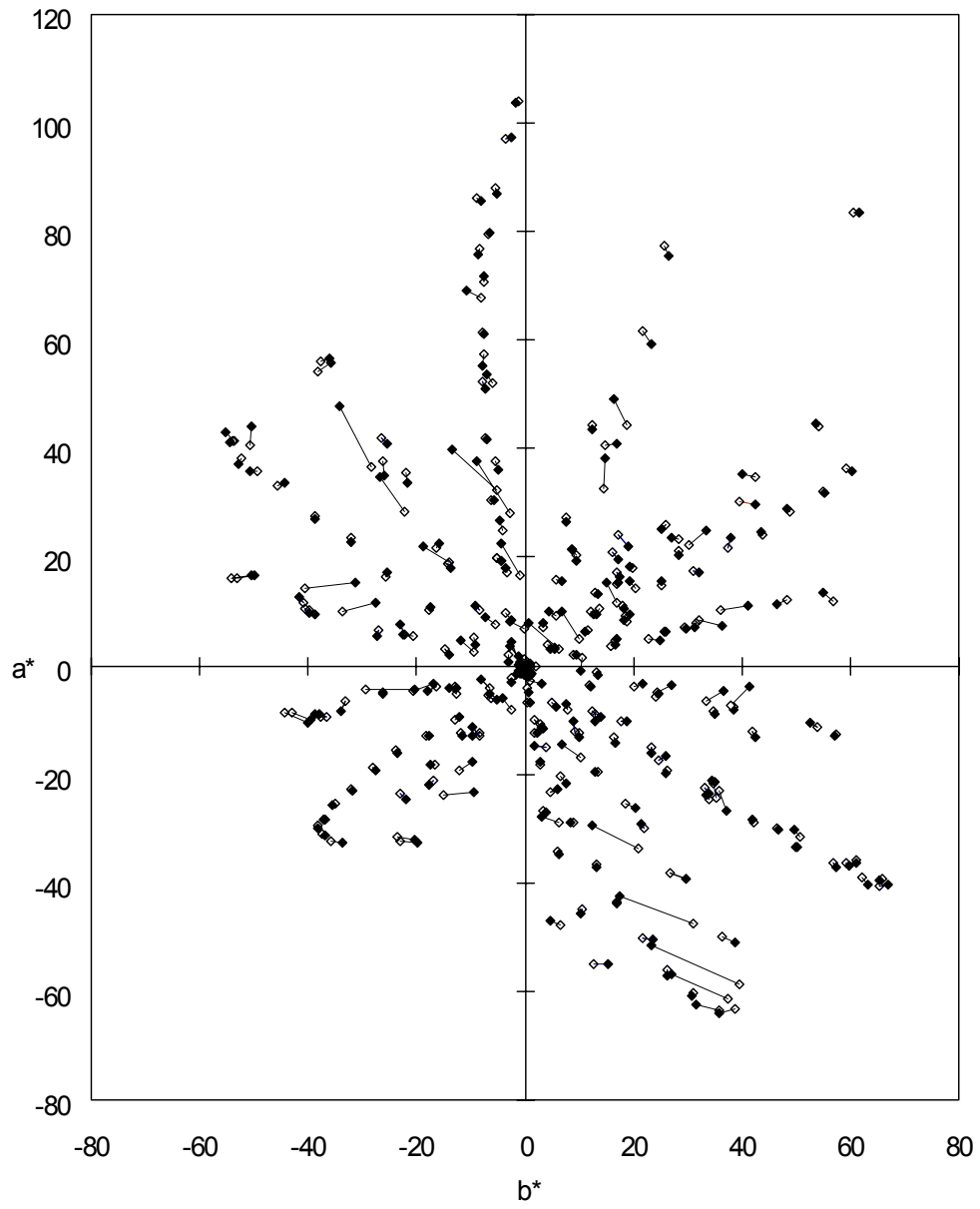


Fig 13.

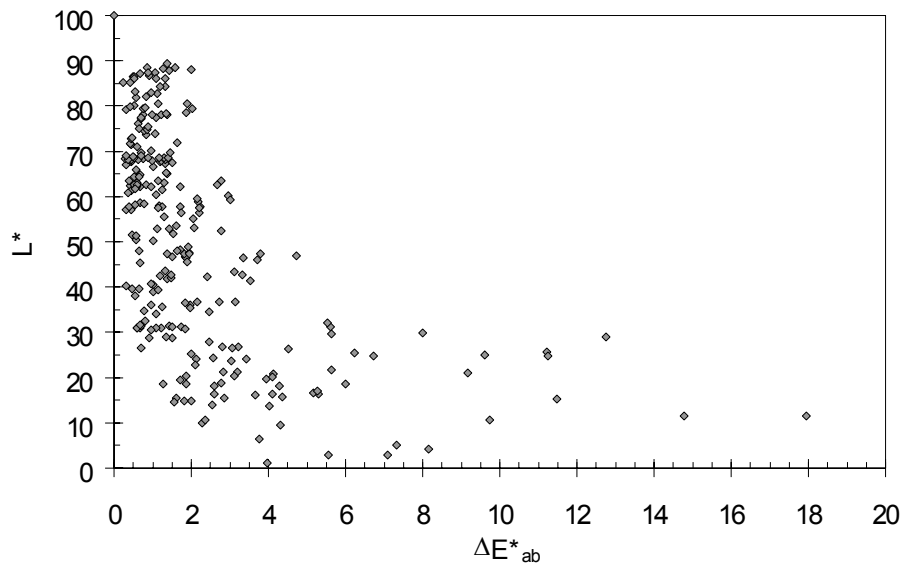


Fig 14.

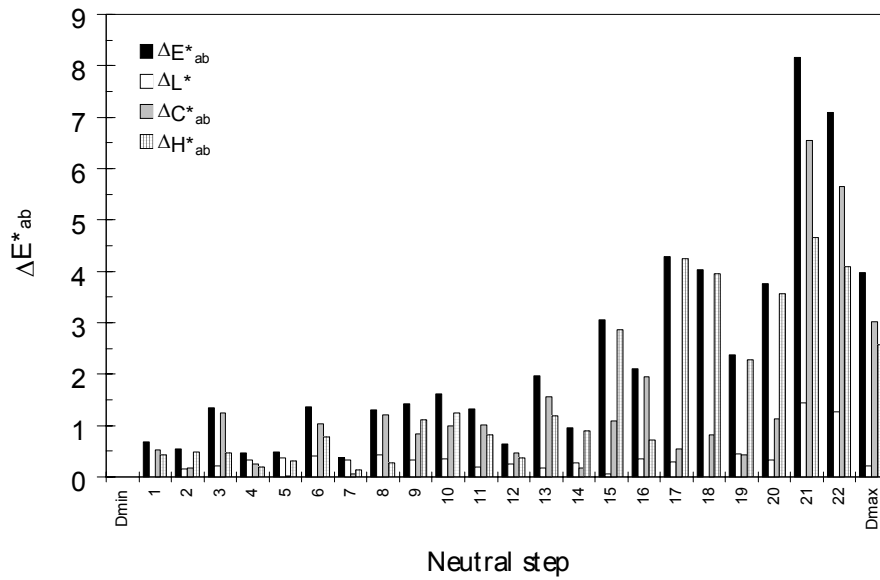


Fig 15.

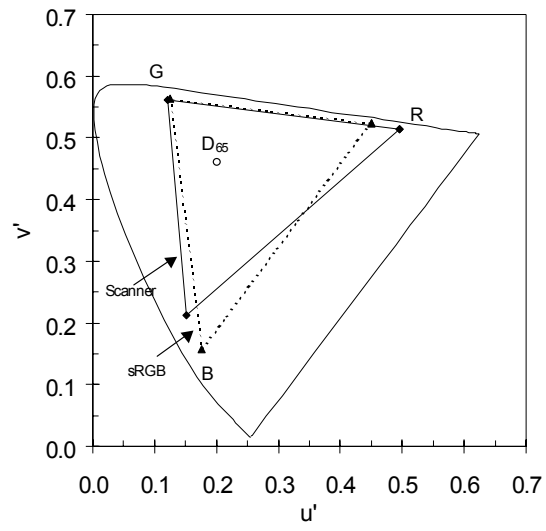
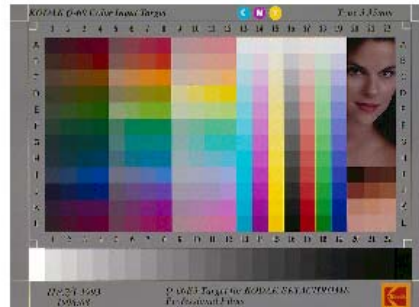
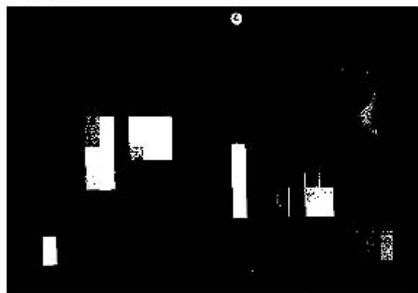


Fig 16.



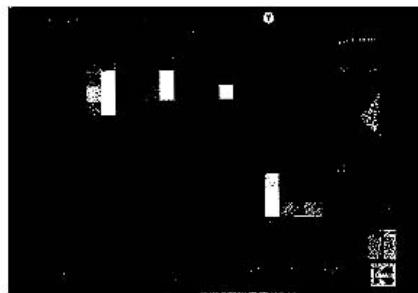
Red



Green



Blue



RGB

